arXiv:2410.23681v2 [math.NA] 1 Nov 2024

Convergent analysis of algebraic multigrid method with data-driven parameter learning for non-selfadjoint elliptic problems

Juan Zhang* and Junyue Luo

Key Laboratory of Intelligent Computing and Information Processing of Ministry of Education, Hunan Key Laboratory for Computation and Simulation in Science and Engineering, School of Mathematics and Computational Science, Xiangtan University, Xiangtan, 411105, Hunan, China.

Contributing authors: zhangjuan@xtu.edu.cn;

Abstract

In this paper, we apply the practical GADI-HS iteration as a smoother in algebraic multigrid (AMG) method for solving second-order non-selfadjoint elliptic problem. Additionally, we prove the convergence of the derived algorithm and introduce a data-driven parameter learing method called Gaussian process regression (GPR) to predict optimal parameters. Numerical experimental results show that using GPR to predict parameters can save a significant amount of time cost and approach the optimal parameters accurately.

Keywords: Elliptic problem, AMG method, Gaussian process regression, convergent analysis

*Corresponding author Juan Zhang. Juan Zhang was partially supported by the National Key R&D Program of China (2023YFB3001604).
Email addresses: zhangjuan@xtu.edu.cn (Juan Zhang*)

1 Introduction

Multigrid methods have effectively tackled the discrete equations that arise from the numerical approximation of elliptic partial differential equations. For self-adjoint positive definite (SPD) problems in particular, multigrid methods have been the focus of extensive research as detailed in [1–9]. In the case of non-self-adjoint and/or indefinite problems, multigrid methods have also been the interest subjects as reported in [10–15]. In this paper, the primary subject of our study is the algebraic multigrid (AMG) method. In 1987, Ruge and Stüben [16] introduced the AMG method, a significant innovation. Unlike traditional geometric multigrid methods, AMG method does not require an understanding of the grid's shape, making it versatile for solving problems with irregular triangulations. Moreover, AMG is applicable to purely discrete problems, including those without a geometric basis, although such situations are rare. Its convenience and effectiveness have led to widespread research and rapid application to specific problems, as discussed in [17–21, 28, 29]. The primary focus of this paper is on the GADI framework [22], where we use it as a new smoother and analyze its convergence. Due to the significant impact of splitting parameters on the efficiency of the algorithm, how to select parameters is also considered in this paper.

There are mainly two traditional approaches to solving the problem of parameter selection. The first involves systematically exploring parameters within a certain range or through experimentation to identify the optimal parameters. This empirical method can yield precise results but is time-consuming. Moreover, in scientific computing, we favor a single, efficient computation over multiple iterations aimed at optimizing algorithm performance. The second approach is to estimate the optimal parameters through theoretical analysis, as suggested in [23]. This method can provide a direct formula or algorithm for calculating the splitting parameters but is contingent on specific problem contexts, and inaccuracies in the estimate can significantly impact algorithm efficiency. Additionally, as the scale of linear systems grows, theoretical methods may become less applicable.

To address these issues, we draw upon the methods outlined in [22], referred to as GPR for predicting optimal parameters. This involves training on a dataset derived from small-scale systems to learn the mapping of relatively optimal splitting parameters in relation to the high dimension of the linear system. This strategy bypasses the need for a costly parameter search and offers an effective means for predicting optimal parameters in practical calculations. In [24], a novel multi-task GPR approach was proposed, along with a kernel learning method for selecting the kernel function. This effectively solves the problem of predicting multiple parameters and enhances the accuracy of predictions.

The rest of this paper is organized as follows. In Section 2, we apply the AMG method to the non-elliptic problem. In Section 3, we use the practical GADI-HS (PGADI-HS) iteration method as a smoother and provide the convergence analysis for the AMG method. In Section 4, we introduce the GPR method to predict the optimal parameter. The numerical examples illustrate that the efficiency of our methods in Section 5. In Section 6, we draw some concluding remark.

Throughout the paper, we use the standard notation for the Sobolev space $W_p^m(\Omega)$, which has a norm$\|\cdot\|_{m,p,\Omega}$ and a seminorm $|\cdot|_{m,p,\Omega}$. For $p=2$, we denote $H^m(\Omega) = W_2^m(\Omega)$, $H_0^1(\Omega) = \{v \in H^1(\Omega) : v|_{\partial\Omega} = 0\}$, $\|\cdot\|_m = \|\cdot\|_{m,2}$ and $\|\cdot\| = \|\cdot\|_{0,2}$. The symbol $x \lesssim y$(or $x \gtrsim y$) indicates that $x \leq Cy$(or $x \geq Cy$), where C is a constant independent of any variable in the inequality.

2 Problem illustration

Consider second-order non-selfadjoint elliptic problem defined by

$$\begin{cases} -\nabla \cdot (a(x)\nabla u) + b(x) \cdot \nabla u + c(x)u = f, & in\ \Omega, \\ u = 0, & on\ \partial\Omega, \end{cases} \tag{1}$$

where Ω is a polygonal domain in R^2, $a(x) \in C^1\left(\overline{\Omega}, R^{2\times 2}\right)$, $b(x) \in C^1\left(\overline{\Omega}\right)^2$, $c(x) \in C^1\left(\overline{\Omega}\right)^2$ and $f \in L^2(\Omega)$. Assume that $a(x) = (\alpha_{ij}(x))_{2\times 2}$ is a uniformly symmetric positive definite matrix on Ω, i.e., there exists a positive constant m_0 such that for any $\xi \in R^2$ and $x \in \overline{\Omega}$, we have $\xi^T a(x)\xi \geq m_0|\xi|^2$. For any $x \in \overline{\Omega}$, as $c(x) - \frac{1}{2}\nabla \cdot b(x) \geq 0$, then (1) has a unique solution. For simplicity, we omit the variable x.

The variational form of (1) is to find $u \in H_0^1(\Omega)$ such that

$$A(u,v) = (f,v), \quad \forall v \in H_0^1(\Omega),$$

where the natural bilinear form is

$$A(u,v) = \int_\Omega (a\nabla u \cdot \nabla v + b \cdot \nabla u v + cuv)\,dx, \quad \forall u, v \in H_0^1(\Omega).$$

The adjoint problem of equation (1) is

$$\begin{cases} -\nabla \cdot (a\nabla u + bu) + cu = f, & in\ \Omega, \\ u = 0, & on\ \partial\Omega. \end{cases}$$

The corresponding variational form is to find $u \in H_0^1(\Omega)$ such that

$$A^*(u,v) \equiv A(u,v) = (f,v), \quad \forall u, v \in H_0^1(\Omega),$$

where the natural bilinear form is

$$A^*(u,v) = \int_\Omega (a\nabla u \cdot \nabla v - b \cdot \nabla u v - \nabla \cdot buv + cuv)\,dx, \quad \forall u, v \in H_0^1(\Omega).$$

Define

$$H(u,v) = \frac{1}{2}(A(u,v) + A^*(u,v)) = \int_\Omega \left(a\nabla u \cdot \nabla v + \left(c - \frac{1}{2}\nabla \cdot b\right)uv\right)dx,$$
$$S(u,v) = \frac{1}{2}(A(u,v) - A^*(u,v)) = \int_\Omega \left(b \cdot \nabla u v + \frac{1}{2}\nabla \cdot buv\right)dx.$$

Obviously, $A(u,v) = H(u,v) + S(u,v)$, and $S(u,v)$ satisfies

$$|S(u,v)| \lesssim \|u\|_1 \|v\|, \quad |S(u,v)| \lesssim \|u\| \|v\|_1, \quad \forall u, v \in H_0^1(\Omega). \tag{2}$$

It is obvious that the operator $H(\cdot,\cdot)$ is positive definite. Thus, we can define the energy norm as $\|u\|_H = \sqrt{H(u,u)}$. Let $\mathscr{T}_k$ $(k = 1, 2, \cdots, J)$ be a sequence of triangulations

on the domain Ω obtained through quasi-uniform refinemen. Let V_k be the piecewise linear finite element space associated with $\mathscr{T}$ and having mesh size h_k, such that

$$V_1 \subset V_2 \subset \cdots \subset V_J \subset H_0^1(\Omega).$$

Define the projection operator P_k: $H_0^1 \longmapsto V_k$ such that

$$A(P_k u, v) = A(u, v), \quad \forall v \in V_k.$$

Lemma 1. [25] *For any given $\epsilon > 0$, there exists an h_0 such that for any $h_k \in (0, h_0)$, we have $\|P_k v\|_1 \lesssim \|v\|_1$ and*

$$\|(I - P_k) v\| \lesssim \epsilon \|(I - P_k) v\|_1, \quad \forall v \in V_k.$$

On each level, define the discrete inner product

$$(u, v)_k = h^2 \sum_{x \in \mathcal{N}_k} u(x) v(x),$$

where $\mathcal{N}_k$ is the set of points on the k-th level grid. For each k, define A_k, H_k and S_k: $V_k \longmapsto V_k$

$$\begin{aligned}
(A_k u, v)_k &= A(u, v), \quad \forall u, v \in V_k, \\
(H_k u, v)_k &= H(u, v), \quad \forall u, v \in V_k, \\
(S_k u, v)_k &= S(u, v), \quad \forall u, v \in V_k.
\end{aligned}$$

Clearly, we have $A_k = H_k + S_k$. Obviously, A_k has an SPD part, namely H_k. Define the grid-related norm $|||\cdot|||_{s,k}$ $(s \in R)$ by

$$|||v|||_{s,k} = \sqrt{(H_k^s v, v)_k} \quad \forall v \in V_k.$$

It is easy to see that $|||v|||_{1,k} = \|v\|_H \approx \|v\|_1$ and $|||v|||_{0,k} = \|v\|$. For simplicity, we define $|||v|||_{1,J} = |||v|||_1$. For any operator $\mathscr{O}$: $V_J \longmapsto V_J$, let $|||\cdot|||_1$ represent its operator norm, i.e.,

$$|||\mathscr{O}|||_1 = \sup_{u,v \in V_J} \frac{|H(\mathscr{O}u, v)|}{|||u|||_1 |||v|||_1}.$$

Define the orthogonal projection operators $\widehat{P}_k$: $H_0^1(\Omega) \longmapsto V_k$ and Q_k: $L^2 \longmapsto V_k$ by

$$H\left(\widehat{P}_k u, v\right) = H(u, v) \quad \forall v \in V_k,$$

$$(Q_k u, v)_k = (u, v) \quad \forall v \in V_k.$$

The k-th level discrete problem of (1) is to find $u_k \in V_k$ such that

$$A(u_k, v) = (f, v) \quad \forall v \in V_k. \tag{3}$$

Hence, the above equation (3) can be written as

$$A_k u_k = f_k,$$

where $f_k = Q_k f$.

Next, we will introduce the simple V-cycle AMG method.

Given $g \in V_k$ and an initial value $u_0 \in V_k$, define an iterative sequence u approximating the true solution by

$$u^{(m+1)} = MG_J(u^m, g), \tag{4}$$

where $MG_J(\cdot, \cdot) : V_J \times V_J \longmapsto V_J$ is a linear mapping defined as follows.

Definition 2.1 Let $MG_1(v,g) = A^{-1}g$, $k > 0$ and $v \in V_k$. Then $MG_k(v,g)$ is defined as

$$MG_k(v,g) = v' + q,$$

where

$$v' = v + R_k(g - A_k v), \quad q = MG_{k-1}(0, P_{k-1}^0(g - A_k v')).$$

$R_k : V_k \longmapsto V_k$ is a linear smoothing operator, the grid transfer operator $P_{k-1}^0 : V_k \longmapsto V_{k-1}$ satisfies

$$\left(P_{k-1}^0 u, v\right)_{k-1} = (u,v)_k, \quad \forall u \in V_k, v \in V_{k-1}.$$

From (4), we can see that $E = MG_J(\cdot, 0)$ is the error reduction operator such that

$$u - u^{m+1} = E\left(u - u^m\right) = MG_J\left(u - u^m, 0\right).$$

Let $T_k = R_k A_k P_k$ for $k > 1$ and $T_1 = P_1$. By the definitions of P^k and P_{k-1}^0, we have

$$P_{k-1}^0 A_k = A_{k-1} P_{k-1}, \quad P_{k-1} P_k = P_{k-1}.$$

The error reduction operator is

$$E = \left(I - T_1\right)\left(I - T_2\right)\cdots\left(I - T_J\right),$$

where I is the identity operator on V_J ([12, 14, 26]).

3 Convergence analysis

In this section, we first apply the PGADI-HS method ([22]) as a smoother in the AMG method and then analyze its convergence.

Consider the linear system

$$Au = f, \quad u \in C^n,$$

where $A \in C^{n\times n}$ is a non-singular matrix. Let

$$A = H + S,$$

where $H = \frac{1}{2}(A + A^*)$, $S = \frac{1}{2}(A - A^*)$, and A^* denotes the conjugate transpose of A.

The iteration format for the PGADI-HS method is as follows.

Given the initial value u^0, for $k = 0, 1, 2, ...$, compute

$$\begin{cases} (\alpha I + H)\, x^{k+\frac{1}{2}} \approx (\alpha I - S)\, x^k + b, \\ (\alpha I + S)\left(x^{k+1} - x^k\right) \approx \alpha\,(2-\omega)\left(x^{k+\frac{1}{2}} - x^k\right). \end{cases} \tag{5}$$

The PGADI-HS method employs the PCG and PCGNE methods in (5). When the residual is very small, consider the iteration (5) as an equality. Then, we can eliminate $x^{k+\frac{1}{2}}$ to obtain

$$(\alpha I + S)\left(x^{k+\frac{1}{2}} - x^k\right) = \alpha\,(2-\omega)\left((\alpha I + H)^{-1}\left((\alpha I - S)\, x^k + b\right) - x^k\right). \tag{6}$$

In order to simplify the above expression, we split the coefficient matrix A as $A = M_1 - N_1 = M_2 - N_2$, where

$$M_1 = \alpha I + H,\ N_1 = \alpha I - S,\ M_2 = \alpha I + S,\ N_2 = \alpha I - H.$$

Then (6) transforms into

$$M_2 x^{k+1} - M_2 x^k = \alpha (2-\omega) \left(M_1^{-1} N_1 x^k + M_1^{-1} b - x^k \right),$$

which implies that

$$x^{k+1} = x^k + \alpha (2-\omega) M_2^{-1} \left(M_1^{-1} N_1 x^k + M_1^{-1} b - x^k \right). \tag{7}$$

Let

$$M(\alpha,\omega) = \tfrac{1}{\alpha(2-\omega)} (\alpha I + H)(\alpha I + S), N(\alpha,\omega) = \tfrac{1}{\alpha(2-\omega)} (\alpha I - H)(\alpha I - S).$$

Obviously, $A = \left(\frac{2-\omega}{2}\right)(M(\alpha,\omega) - N(\alpha,\omega))$. Then we can rewrite equation (7) as

$$\begin{aligned} x^{k+1} &= x^k + M(\alpha,\omega)^{-1} N_1 x^k - M(\alpha,\omega)^{-1} M_1 x^k + M(\alpha,\omega)^{-1} b \\ &= x^k + M(\alpha,\omega)^{-1} \left((-M_1 + N_1) x^k + b \right) \\ &= x^k + M(\alpha,\omega)^{-1} \left(-A x^k + b \right). \end{aligned}$$

From the above analysis, the smoothing operator is

$$R_k = \alpha (2-\omega) (\alpha I + S_k)^{-1} (\alpha I + H_k)^{-1}.$$

3.1 SPD problem

Next, we divide the convergence analysis into self-adjoint positive definite case and non-selfadjoint positive definite case. We first analyze the self-adjoint positive definite case.

For the k-th level problem, we define $\widehat{R}_k$ as the smoother at level k. The following regularity conditions are required.

Condition 1. *There exists a constant $\omega > 0$ independent of J and the grid size h_k such that*

$$\frac{\omega}{\lambda_k} (v,v)_k \le \left(\bar{R}_k v, v \right)_k, \forall v \in V_k, \tag{8}$$

where $\bar{R}_k = \widehat{R}_k + \widehat{R}_k^T - \widehat{R}_k^T H_k \widehat{R}_k$ and λ_k is the maximum eigenvalue of H_k. It is easy to see that $\lambda_k \approx h_k^{-2}$.

Condition 2. *There exists a constant $\theta \in (0,2)$ independent of J and the grid size h_k, such that:*

$$H\left(\hat{R}_k v, \hat{R}_k v \right) \le \theta \left(\hat{R}_k v, v \right)_k, \forall v \in V_k. \tag{9}$$

If inequality (9) is satisfied, then (8) is equivalent to

$$\frac{1}{\lambda_k} (v,v)_k \lesssim \left(\hat{R}_k v, v \right)_k, \forall v \in V_k. \tag{10}$$

Consider the SPD problem defined by

$$H_k u_k = b_k. \tag{11}$$

Correspondingly,

$$\begin{aligned}\hat{R}_k &= \alpha\left(2-\omega\right)\left(\alpha I + S_k\right)^{-1}\left(\alpha I + H_k\right)^{-1} \\ &= \alpha\left(2-\omega\right)\left(\alpha I\right)^{-1}\left(\alpha I + H_k\right)^{-1} \\ &= \left(2-\omega\right)\left(\alpha I + H_k\right)^{-1}. \end{aligned} \tag{12}$$

The error reduction operator for the SPD problem (11) is given by

$$\hat{E}_J = \left(I - \hat{T}_1\right)\left(I - \hat{T}_2\right)\cdots\left(I - \hat{T}_J\right). \tag{13}$$

where for all $\forall k > 1, \hat{T}_k = \hat{R}_k H_k \hat{P}_k$ and $\hat{T}_1 = \hat{P}_1$.

Lemma 2. [3] For $k > 1$, assuming $\hat{R}_k$ satisfies Conditions 1 and 2. Hence there exists a constant $\hat{\delta} < 1$ independent of J such that

$$H\left(\hat{E}u, \hat{E}u\right) \leq \hat{\delta}^2 H\left(u, u\right), \forall u \in V_J.$$

From Lemma 2 and the definition of the norm $|||\cdot|||_1$, we have $\left|\left|\left|\hat{E}\right|\right|\right|_1 \leq \hat{\delta}$.

Theorem 1. *For $k > 1$, let $\hat{R}_k$ satisfy the definition of (12) and assume $\omega \in (0, 2)$, $\alpha > -\frac{\omega\lambda_k}{2}$. Under the assumptions stated earlier, there exists a constant $\hat{\delta} < 1$ independent of J such that*

$$\left|\left|\left|\hat{E}\right|\right|\right|_1 \leq \hat{\delta}.$$

Proof. By Lemma 2, it is only required to verify $\hat{R}_k$ satisfies Conditions 1 and 2. From (12), we have

$$\begin{aligned} H\left(\hat{R}_k v, \hat{R}_k v\right) &= H\left(\left(2-\omega\right)\left(\alpha I + H\right)^{-1} v, \left(2-\omega\right)\left(\alpha I + H\right)^{-1} v\right) \\ &= \left(\left(2-\omega\right)\left(\alpha I + H\right)^{-1} v, \left(2-\omega\right) H_k \left(\alpha I + H\right)^{-1} v\right)_k \\ &\leq \frac{\left(2-\omega\right)\lambda_k}{\alpha + \lambda_k}\left(\hat{R}_k v, v\right)_k \\ &= \theta\left(\hat{R}_k v, v\right)_k. \end{aligned}$$

Based on the assumption, this shows that the Condition 2 is met, where

$$\theta = \frac{\left(2-\omega\right)\lambda_k}{\alpha + \lambda_k} = \frac{2-\omega}{\frac{\alpha}{\lambda_k} + 1} < 2.$$

Furthermore, as

$$\left(\hat{R}_k v, v\right)_k = \left(\left(2-\omega\right)\left(\alpha I + H\right)^{-1} v, v\right)_k \geq \frac{2-\omega}{\frac{\alpha}{\lambda_k} + 1}\frac{1}{\lambda_k}\left(v, v\right)_k = C\frac{1}{\lambda_k}\left(v, v\right)_k,$$

where $C > 0$ is a constant. Therefore, Condition 1 is also satisfied, completing the proof. □

Note that we assume $\alpha > -\frac{\omega\lambda_k}{2}$, where α is negative. In numerical computation, take $\alpha > 0$ as a matter of convention.

3.2 Non-selfadjoint problem

For the non-selfadjoint problem, the analysis is based on the error perturbation estimate.

Lemma 3. [27] *Let $E_k = (I - T_1)(I - T_2)\cdots(I - T_k)$ satisfy the definition (2), $\hat{E}_k = \left(I - \hat{T}_1\right)\left(I - \hat{T}_2\right)\cdots\left(I - \hat{T}_k\right)$ satisfy the definition (13), and*

$$\left|\left|\left|I - \hat{T}_k\right|\right|\right|_1 \leq 1, \left|\left|\left|T_k - \hat{T}_k\right|\right|\right|_1 \lesssim h_k, k = 2, ..., J.$$

Then, given $\epsilon > 0$, there exists $h_0(\epsilon) > 0$ and $C > 0$, such that for $h_1 \leq h_0(\epsilon)$, we have

$$|||E|||_1 \leq \left|\left|\left|\hat{E}\right|\right|\right|_1 + C(h_1 + \epsilon).$$

Theorem 2. *Let R_k be defined as in (3), assuming $\omega \in (0, 2)$, $\alpha > -\frac{\omega\lambda_k}{2}$. Given $\epsilon > 0$, there exists $h_0(\epsilon) > 0$ such that for $h_1 \leq h_0(\epsilon)$, we have*

$$|||E|||_1 \leq \left|\left|\left|\hat{E}\right|\right|\right|_1 + C(h_1 + \epsilon),$$

where $C > 0$ is a constant, $\hat{E}$ is defined in (13).

Proof. Consider the perturbation operator $T_k - \hat{T}_k$ and the norm $\left|\left|\left|T_k - \hat{T}_k\right|\right|\right|_1$, where

$$T_k = R_k A_k P_k, \quad \hat{T}_k = \hat{R}_k H_k \hat{P}_k.$$

From inequality (9), we have $\left|\left|\left|\hat{T}_k\right|\right|\right|_1 \leq \theta$. Therefore, for all $\forall w \in V_J$, we get

$$\begin{aligned} H\left(\left(I - \hat{T}_k\right)w, \left(I - \hat{T}_k\right)w\right) &= H(w, w) - 2H\left(\hat{T}_k w, w\right) + H\left(\hat{T}_k w, \hat{T}_k w\right) \\ &\leq H(w, w) - 2H\left(\hat{T}_k w, w\right) + \theta H\left(\hat{T}_k w, w\right) \\ &= H(w, w) - (2 - \theta) H\left(\hat{T}_k w, w\right) \\ &\leq H(w, w). \end{aligned}$$

This implies that

$$\left|\left|\left|I - \hat{T}_k\right|\right|\right|_1 \leq 1. \tag{14}$$

For $k \geq 2$, we consider the perturbation operator

$$\begin{aligned} T_k - \hat{T}_k &= R_k A_k P_k - \hat{R}_k H_k \hat{P}_k \\ &= (2 - \omega)\alpha(\alpha I + S_k)^{-1}(\alpha I + H_k)^{-1} A_k P_k - (2 - \omega)(\alpha I + H_k)^{-1} H_k \hat{P}_k \\ &= \alpha(\alpha I + S_k)^{-1}\left(\hat{R}_k A_k P_k - \hat{R}_k H_k \hat{P}_k + \hat{R}_k H_k \hat{P}_k\right) - (2 - \omega)(\alpha I + H_k)^{-1} H_k \hat{P}_k \\ &= \alpha(\alpha I + S_k)^{-1}\left(\hat{R}_k A_k P_k - \hat{R}_k H_k \hat{P}_k\right) + (2 - \omega)\alpha(\alpha I + S_k)^{-1}(\alpha I + H_k)^{-1} H_k \hat{P}_k \\ &\quad - (2 - \omega)(\alpha I + H_k)^{-1} H_k \hat{P}_k \end{aligned}$$

$$
\begin{aligned}
&= \alpha\left(\alpha I + S_k\right)^{-1}\left(\hat{R}_k A_k P_k - \hat{R}_k H_k \hat{P}_k\right) + (2-\omega)\left(\left(\alpha\left(\alpha I + S_k\right)^{-1} - I\right)\left(\alpha I + H_k\right)^{-1}\right) H_k \hat{P}_k \\
&= \alpha\left(\alpha I + S_k\right)^{-1}\left(\hat{R}_k A_k P_k - \hat{R}_k H_k \hat{P}_k\right) + \left(\left(\alpha I + S_k\right)^{-1}\alpha - \left(\alpha I + S_k\right)^{-1}\left(\alpha I + S_k\right)\right)\hat{R}_k H_k \hat{P}_k \\
&= \alpha\left(\alpha I + S_k\right)^{-1}\left(\hat{R}_k A_k P_k - \hat{R}_k H_k \hat{P}_k\right) - \left(\alpha I + S_k\right)^{-1} S_k \hat{R}_k H_k \hat{P}_k \\
&= \alpha\left(\alpha I + S_k\right)^{-1}\left(\hat{R}_k A_k P_k - \hat{R}_k H_k \hat{P}_k\right) - \left(\alpha I + S_k\right)^{-1} S_k \hat{T}_k. \qquad (15)
\end{aligned}
$$

By the definition of the projection operators P_k, $\hat{P}_k$, we get

$$
\begin{aligned}
H\left(\hat{R}_k A_k P_k w, v\right) &= \left(\hat{R}_k A_k P_k w, H_k \hat{P}_k v\right)_k \\
&= \left(A_k P_k w, \hat{R}_k H_k \hat{P}_k v\right)_k \\
&= A\left(w, \hat{T}_k v\right) \\
&= H\left(w, \hat{T}_k v\right) + S\left(w, \hat{T}_k v\right) \\
&= H\left(\hat{T}_k w, v\right) + S\left(w, \hat{T}_k v\right).
\end{aligned}
$$

From the above equation, we have

$$
H\left(\left(\hat{R}_k A_k P_k - \hat{R}_k H_k \hat{P}_k\right) w, v\right) = S\left(w, \hat{T}_k v\right), \forall w, v \in V_J.
$$

Using (2), hence

$$
\left|H\left(\left(\hat{R}_k A_k P_k - \hat{R}_k H_k \hat{P}_k\right) w, v\right)\right| \lesssim |||w|||_1 \left\|\hat{T}_k v\right\|. \qquad (16)
$$

Since for all $\forall v \in V_k$, it is evident that

$$
h^{-2} \approx \lambda_k, \quad \left(\hat{R}_k v, v\right)_k \leq C\lambda_k^{-1}\left(v, v\right)_k.
$$

In terms of (2), then

$$
\begin{aligned}
\left\|\hat{T}_k v\right\| &\approx \left(\hat{R}_k H_k \hat{P}_k v, \hat{R}_k H_k \hat{P}_k v\right)_k^{\frac{1}{2}} \leq C\lambda_k^{-\frac{1}{2}}\left(\hat{R}_k H_k \hat{P}_k v, H_k \hat{P}_k v\right)_k^{\frac{1}{2}} \\
&= C\lambda_k^{-\frac{1}{2}} H\left(\hat{R}_k H_k \hat{P}_k v, \hat{P}_k v\right)_k^{\frac{1}{2}} \\
&\lesssim h_k H\left(\hat{T}_k v, v\right)^{\frac{1}{2}} \lesssim h_k \left|||\hat{T}_k|||_1 H\left(v, v\right)^{\frac{1}{2}} \right. \\
&\lesssim h_k |||v|||_1. \qquad (17)
\end{aligned}
$$

Combining (16) and (17) yields

$$\left|\left|\left|\left(\hat{R}_k A_k P_k - \hat{R}_k H_k \hat{P}_k\right)\right|\right|\right| \lesssim h_k. \tag{18}$$

By (2), we get

$$\begin{aligned} H\left(S_k\hat{P}_k w, v\right) &= \left(S_k\hat{P}_k w, H_k\hat{P}_k v\right)_k \\ &= S\left(\hat{P}_k w, H_k\hat{P}_k v\right) \\ &\lesssim |||w|||_1 \left|\left|H_k\hat{P}_k v\right|\right|, \forall w, v \in V_J. \end{aligned} \tag{19}$$

Obviously,

$$\lambda_k^{-1}\left|\left|H_k\hat{P}_k v\right|\right| \approx \lambda_k^{-1}\left(H_k\hat{P}_k v, H_k\hat{P}_k v\right)_k^{\frac{1}{2}} = \lambda_k^{-\frac{1}{2}} H\left(v, \lambda_k^{-1} H_k\hat{P}_k v\right)^{\frac{1}{2}} \lesssim h_k |||v|||_1. \tag{20}$$

Using (19), (20), and the definition of $|||\cdot|||_1$ norm, we have

$$\lambda_k^{-1} |||S_k|||_1 \lesssim h_k. \tag{21}$$

By Neumann lemma and (21), we get

$$\left|\left|\left|\alpha\left(\alpha I + S_k\right)^{-1}\right|\right|\right|_1 = \left|\left|\left|\left(I + \alpha^{-1} S_k\right)^{-1}\right|\right|\right|_1 \leq C, \tag{22}$$

$$\left|\left|\left|\left(\alpha I + S_k\right)^{-1} S_k\right|\right|\right|_1 = \left|\left|\left|\left(I + \alpha^{-1} S_k\right)^{-1} \alpha^{-1} S_k\right|\right|\right|_1 \lesssim h_k. \tag{23}$$

Combining (15), (18), (22) with (23), we have

$$\begin{aligned} \left|\left|\left|T_k - \widehat{T}_k\right|\right|\right|_1 \leq & \left|\left|\left|\alpha\left(\alpha I + S_k\right)^{-1}\right|\right|\right|_1 \left|\left|\left|\widehat{R}_k A_k P_k - \widehat{R}_k H_k \widehat{P}_k\right|\right|\right|_1 \\ & + \left|\left|\left|\left(\alpha I + S_k\right)^{-1} S_k\right|\right|\right|_1 \left|\left|\left|\widehat{T}_k\right|\right|\right|_1 \\ & \lesssim h_k. \end{aligned}$$

Considering Lemma 3, we complete the proof. □

4 Parameter selection

In this section, we use Gaussian Process Regression (GPR) derived in [22, 24] to predict optimal parameters.

4.1 GPR

Suppose the training set is $D = \{(n_i, \alpha_i)|i = 1, 2, \cdots, d\} := \{\boldsymbol{n}, \boldsymbol{\alpha}\}$, where (n_i, α_i) are input-output pairs. If α_i follows a Gaussian Process (GP) relative to n_i, then $f(n) = [f(n_1), f(n_2), \cdots, f(n_d)]$ follows a d-dimensional Gaussian distribution (GD)

$$\begin{bmatrix} f(n_1) \\ \vdots \\ f(n_d) \end{bmatrix} \sim N\left(\begin{bmatrix} \mu(n_1) \\ \vdots \\ \mu(n_d) \end{bmatrix}, \begin{bmatrix} k(n_1, n_1) & \cdots & k(n_1, n_d) \\ \vdots & \ddots & \vdots \\ k(n_d, n_1) & \cdots & k(n_d, n_d) \end{bmatrix} \right).$$

Clearly, GP is determined by the mean function $\mu(n)$ and the covariance function $k(n, n')$. We can then express the GP as follows

$$f(n) \sim GP\left(\mu(n), K(n, n')\right),$$

where n, n' are any two random variables in the input set $\boldsymbol{n}$, and typically, we set the mean function to 0.

The purpose of Gaussian Process Regression (GPR) is to learn the mapping relationship between the input set $\boldsymbol{n}$ and the output set $\boldsymbol{\alpha}$, that is, $f(n) : \mathbb{R} \to \mathbb{R}$, and to infer the possible output value $\alpha_* = f(n_*)$ for a test point n_*. In practical linear regression problems, the model we consider is

$$\alpha = f(n) + \eta,$$

where α is the observed value affected by noise η. Additionally, we assume that η follows a d-dimensional Gaussian joint distribution with mean 0 and variance σ^2, that is, $\eta \sim N(0, \sigma^2)$. The ideal range for σ is $[10^{-6}, 10^{-2}]$. In this paper, we set $\sigma = 10^{-4}$.

Then, we can express the prior distribution of the observed values $\boldsymbol{\alpha}$ as follows

$$\boldsymbol{\alpha} \sim N\left(\boldsymbol{\mu}_\alpha(\boldsymbol{n}), K(\boldsymbol{n}, \boldsymbol{n}) + \sigma^2 I_d\right)$$

The joint prior distribution of the observed values θ and the predictive values θ_* is given by

$$\begin{bmatrix} \boldsymbol{\alpha} \\ \boldsymbol{\alpha}_* \end{bmatrix} \sim N\left(\begin{bmatrix} \boldsymbol{\mu}_\alpha \\ \boldsymbol{\mu}_{\alpha_*} \end{bmatrix}, \begin{bmatrix} K(\boldsymbol{n}, \boldsymbol{n}) + \sigma^2 I_d & K(\boldsymbol{n}, \boldsymbol{n}_*) \\ K(\boldsymbol{n}_*, \boldsymbol{n}) & K(\boldsymbol{n}_*, \boldsymbol{n}_*) \end{bmatrix} \right),$$

Where I_d is the d-th order identity matrix, $K(\boldsymbol{n}, \boldsymbol{n}) = (k_{ij})$ is the symmetric positive definite covariance matrix with $k_{ij} = k(n_i, n_j)$. Additionally, $K(\boldsymbol{n}, \boldsymbol{n}_*)$ represents the symmetric covariance matrix between the training set N and the test set $\boldsymbol{n}_*$.

According to Bayes' theorem

$$p(\boldsymbol{\alpha}_*|\boldsymbol{\alpha}) = \frac{p(\boldsymbol{\alpha}|\boldsymbol{\alpha}_*)\, p(\boldsymbol{\alpha}_*)}{p(\boldsymbol{\alpha})},$$

The predicted joint posterior distribution is

$$\boldsymbol{\alpha}_*|\boldsymbol{n}, \boldsymbol{\alpha}, \boldsymbol{n}_* \sim N\left(\boldsymbol{\mu}_*, \boldsymbol{\sigma}_*^2\right),$$

where

$$\begin{aligned} \boldsymbol{\mu}_* &= K(\boldsymbol{n}_*, \boldsymbol{n}) \left[K(\boldsymbol{n}, \boldsymbol{n}) + \sigma^2 I_d\right]^{-1} (\boldsymbol{\alpha} - \boldsymbol{\mu}_\alpha) + \boldsymbol{\mu}_{\alpha_*}, \\ \boldsymbol{\sigma}_*^2 &= K(\boldsymbol{n}_*, \boldsymbol{n}_*) - K(\boldsymbol{n}_*, \boldsymbol{n}) \left[K(\boldsymbol{n}, \boldsymbol{n}) + \sigma^2 I_d\right]^{-1} K(\boldsymbol{n}, \boldsymbol{n}_*). \end{aligned}$$

For the outputs α_* in the test set, we can use the mean of the aforementioned Gaussian regression as its estimated value. That is, $\widehat{\alpha}_* = \mu_*$. The kernel function is crucial to the GPR method, as it generates the covariance matrix that measures the distance between any two input variables. The closer the distance, the higher the correlation

between the corresponding output variables. Therefore, it is necessary to select or construct a kernel function based on actual needs. The most commonly used kernel functions include the Radial Basis Function, Rational Quadratic kernel, Exponential (or Matern) kernel, and Periodic kernel. More kernel functions can be referenced in [22]. In this work, we choose the Gaussian kernel function

$$\kappa(x,y) = \sigma_f^2 \exp\left(\frac{-\|x-y\|}{2\iota^2}\right),$$

where $\theta = \{\iota, \sigma_f\}$ is referred to as the hyperparameters. The optimal hyperparameters are obtained through the maximum likelihood estimation function, which is given by:

$$L = \log p(y|x,\theta) = -\tfrac{1}{2} y^T \left[K + \sigma^2 I_d\right]^{-1} - \tfrac{1}{2}\log\left[K + \sigma^2 I_d\right] - \tfrac{n}{2}\log 2\pi.$$

4.2 Multitask GPR

For multi-task prediction problems, [24] proposed a multi-task GPR method, which learns M correlated functions $f_l, l = 1, ..., M$ from the dataset $\{(\boldsymbol{x}_{li}, y_{li})|l = 1, ..., M, i = 1, ..., n, \boldsymbol{x}_{li} \in \mathbb{R}^d, y_{li} \in \mathbb{R}\}$ to avoid singularity, we consider the following noisy model

$$y_{li} = f_l(\boldsymbol{x}_{li}) + \epsilon_l, \epsilon_l \sim \mathcal{N}\left(0, \sigma_l^2\right), \tag{24}$$

Where $y_{li}(x_{li})$ is the i-th output (input) for the l-th task, and ϵ_l is the white noise for the l-th task.

Let $\boldsymbol{y} = [y_{11}, \cdots, y_{1n}, \cdots, y_{M1}, \cdots, y_{Mn}]^T = \text{vec}\left(Y^T\right)$ be the output vector, and $\boldsymbol{f} = [\, f_1, \cdots, f_1, \cdots, f_M, \cdots, f_M\,]^T = \text{vec}\left(F^T\right)$ be the vector of latent functions. The multi-task regression problem can be formulated as a Gaussian Process prior for the latent functions

$$f \sim GP(0, K^t \otimes K^x),$$

where $K^t \in \mathbb{R}^{M\times M}$ and $K^x \in \mathbb{R}^{n\times n}$ are the covariance matrices for tasks and data, respectively. The noise model (24) becomes

$$\boldsymbol{y} \sim \mathcal{N}(0, K^t \otimes K^x + D \otimes I_n),$$

where $D = \text{diag}\left[\sigma_1^2, \cdots, \sigma_M^2\right] \in \mathbb{R}^{M\times M}$. The predictive distribution for the l-th task at a new point x_* given $\boldsymbol{y}$ is

$$\boldsymbol{y}_*|\boldsymbol{y} \sim \mathcal{N}(\mu_{*l}, \Sigma_{*l}),$$

where

$$\begin{aligned}
&\mu_{*l} = \left(k_l^t \otimes k^x_{\boldsymbol{x},\boldsymbol{x}_*}\right)^T \Sigma^{-1}\boldsymbol{y},\\
&\Sigma_{*l} = k_{ll}^t k^x_{\boldsymbol{x},\boldsymbol{x}_*} - \left(k_l^t \otimes k^x_{\boldsymbol{x},\boldsymbol{x}_*}\right)^T \Sigma^{-1}\left(k_l^t \otimes k^x_{\boldsymbol{x},\boldsymbol{x}_*}\right),\\
&\Sigma = K^t \otimes K^x + D \otimes I_n.
\end{aligned}$$

k_{ll}^t and k_l^t represent the l-th diagonal element and the l-th column of K^t, respectively. $k^x_{\boldsymbol{x},\boldsymbol{x}_*}$ is the covariance between the test point $\boldsymbol{x}_*$ and the training point $\boldsymbol{x}$. The hyperparameters θ^t and θ^x appear in the task covariance function and the data covariance function, respectively. To obtain the hyperparameter estimates, we employ the L-BFGS method to maximize the log form of the marginal likelihood function L

$$L = \log p(\boldsymbol{y}|\boldsymbol{x},\theta_x,\theta_t) = -\frac{n}{2}\log\left|K^t\right| - \frac{M}{2}\log|K^x| - \frac{1}{2}trace\left[\left(K^t\right)^{-1} F^T \left(K^x\right)^{-1} F\right]$$

$$-\frac{n}{2}\sum_{l=1}^{M}\log\sigma_l^2-\frac{1}{2}trace\left[\left(Y-F\right)D^{-1}\left(Y-F\right)^T\right]-\frac{Mn}{2}\log 2\pi.$$

[24] proposed a method for selecting kernel functions. A kernel function library $\mathcal{K}=\{k_\xi(x,x')|\xi=1,\cdots,N\}$ is provided, which includes basic kernel functions and their multiplicative combinations. For the l-th training task, $l=1,\cdots,M$, the kernel function used is a linear combination of the elements in the kernel function library

$$k\left(x,x'\right)=\sum_{\xi=1}^{N}c_{l\xi}k_\xi\left(x,x'\right).$$

For N training tasks, the weighted matrix is

$$C=\begin{bmatrix}c_{11}&\cdots&c_{1N}\\ \vdots&\ddots&\vdots\\ c_{M1}&\cdots&c_{MN}\end{bmatrix}.$$

It should be noted that, in the GPR method, the training data comes from smaller systems, i.e., small data sets. Learning kernel functions from small data through (deep) neural networks is difficult. Therefore, we predetermine the kernel library instead of directly learning the kernel functions from the data.

5 Numerical examples

In this section, we will provide three numerical examples to illustrate the performance of the proposed smoother in AMG method and demonstrate the parameter selection method. The numerical experiments are implemented based on the IFEM toolbox.

Example 5.1 Consider the following 2D Poisson equation

$$\begin{cases}-\nabla\left(\nabla u\right)=f, & (x,y)\in\Omega=\left[-\frac{\pi}{6},\frac{\pi}{6}\right]\times[0,1],\\ u=0, & (x,y)\in\partial\Omega.\end{cases}$$

The exact solution is given by

$$u=\frac{1}{9+\pi^2}\cos(3x)\sin(\pi y),$$

with the right-hand side derived from the exact solution.

We solve the problem using the AMG method, with the coarsening scheme chosen as the RS coarsening and the connectivity parameter selected as 0.025. The initial guess for iteration is 0. If the relative residual satisfies

$$res=\frac{\left\|r^k\right\|_2}{\left\|r^0\right\|_2}\leq 10^{-8},$$

where $r^k=b-Au^k$, the iteration is terminated. Choose PGADI-HS method as the smoother in the AMG method. The internal systems solved using the CG and CGNE methods, and the preconditioning matrix $M=I$. In a simple traversal, we found that the algorithm is not sensitive to ω, with the optimal ω being 1.9. We then traverse α in the interval $(0,0.1]$ with a step size of 0.001. For the AMG method using the HSS method as the smoother, we obtain the parameters using the formula for the optimal

parameter selection of the HSS method. Below is a comparison of the AMG method results using two different types of smoothers:

Table 1 Comparison of AMG method with different smoothing algorithms(Example 5.1).

	PGADI-HS Method				HSS Method		
n	(α,ω)	$iter$	$cputime$	$traversal\ \ cputime$	α	$iter$	$cputime$
16	(0.079,1.9)	4	0.004	49.701	0.7812	13	0.035
32	(0.074,1.9)	6	0.025	168.861	0.3925	26	0.146
48	(0.070,1.9)	9	0.070	304.186	0.2619	39	0.900
64	(0.068,1.9)	12	0.169	719.673	0.1965	54	4.385
96	(0.067,1.9)	16	0.762	1959.528	0.1310	83	36.109
128	(0.065,1.9)	22	1.250	2711.728	0.0982	112	141.222

We use the GPR algorithm to predict the splitting parameter α of the smoothing algorithm. The table below presents the training set, test set, and retraining set for GPR. For small-scale linear systems, n ranges from 4 to 160 with a step size of $\Delta n = 4$ to obtain the training set. For the test set, we use a step size of $\Delta n = 1$, ranging from 1 to 216. In the retraining set, we use a step size of $\Delta n = 4$ and n ranges from 70 to 216.

Table 2 Training set, test set, and retraining set for the PGADI-HS smoothing algorithm in the algebraic multigrid method using GPR(Example 5.1).

training set	$n : 4 \sim 160, \Delta n = 4$	test set	$n : 1 \sim 216, \Delta n = 1$	retraining set	$n : 70 \sim 216, \Delta n = 4$

Fig. 1 Regression curve of α with respect to n in the PGADI-HS smoothing algorithm of the AMG method(Example 5.1).

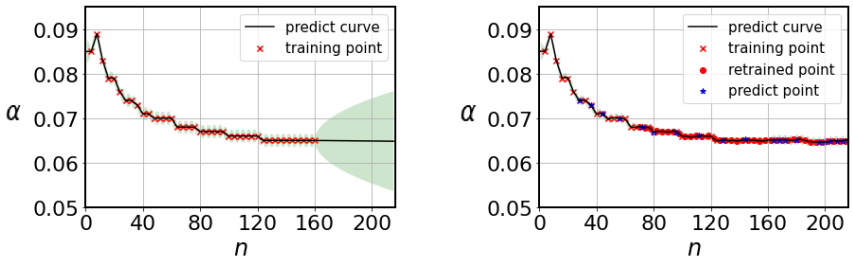

The table below presents the numerical results of solving the two-dimensional Poisson equation using AMG method with the PGADI-HS smoothing algorithm (obtained through the GPR algorithm for the optimal parameter α):

Using the GPR algorithm, we can obtain relatively optimal parameters is clearly much more efficient compared to obtaining them through exhaustive search.

Example 5.2 Consider the following equation

Table 3 Prediction results using AMG with the PGADI-HS smoother(Example 5.1).

n	(α,ω)	$iter$	$cputime$	n	(α,ω)	$iter$	$cputime$
28	(0.0739,1.9)	6	0.022	36	(0.0729,1.9)	7	0.020
44	(0.0711,1.9)	8	0.033	56	(0.0699,1.9)	10	0.067
72	(0.0679,1.9)	13	0.167	80	(0.0668,1.9)	15	0.230
96	(0.0668,1.9)	16	0.416	112	(0.0661,1.9)	19	0.725
128	(0.0650,1.9)	22	1.078	144	(0.0651,1.9)	23	1.439
164	(0.0651,1.9)	26	2.990	168	(0.0651,1.9)	27	3.253
172	(0.0651,1.9)	28	3.571	180	(0.0651,1.9)	29	3.977
196	(0.0646,1.9)	31	5.018	200	(0.0646,1.9)	31	5.149
204	(0.0648,1.9)	32	6.638	208	(0.0648,1.9)	32	6.692
212	(0.0649,1.9)	33	7.510	216	(0.0650,1.9)	33	7.345

$$\begin{cases} -\Delta u + ku = f, & (x,y) \in \Omega = [0,1] \times [0,1], \\ u = 0, & (x,y) \in \partial\Omega. \end{cases}$$

The exact solution is given by $u = x(1-x)\sin(\pi y)$, with the coefficient taken as $k = 0.2$, and the right-hand side is derived from the exact solution. We set up Example 5.2 in the same way as Example 5.1. In a simple traversal, it is found that the algorithm is sensitive to the changes in both α and ω. Below, we traverse to obtain the optimal parameters by setting α in the interval $(0, 1]$ with a step size of 0.01, and setting ω in the interval $(0.5, 1.5]$ with a step size of 0.05; for the AMG method using the HSS method as the smoother, we use the formula for the optimal parameter selection of the HSS method to obtain the parameters. The following is a comparison of the AMG method results using two different types of smoothers:

Table 4 Comparison of the AMG method with different smoothing algorithms(Example 5.2).

	PGADI-HS Method					HSS Method		
n	(α,ω)	$iter$	$cputime$	$traversal$	$cputime$	α	$iter$	$cputime$
16	(0.76,0.90)	6	0.004	45.736		0.7507	13	0.012
32	(0.53,1.20)	10	0.021	192.452		0.3859	26	0.131
48	(0.49,1.25)	11	0.046	633.677		0.2593	39	0.953
64	(0.38,1.40)	21	0.193	1804.820		0.1952	53	4.182
96	(0.38,1.40)	25	0.516	8174.274		0.1306	82	30.907
128	(0.35,1.45)	36	2.735	30933.853		0.0981	111	132.201

We use the GPR algorithm to predict the splitting parameters (α,ω). The table below provides the training set, test set, and retraining set for GPR. For small-scale linear systems, we set n ranging from 8 to 160 with a step size of $\Delta n = 4$ to obtain the training set. For the test set, we choose a step size of $\Delta n = 1$, with n ranging from 1 to 220. In the retraining set, we select a step size of $\Delta n = 10$, with n ranging from 170 to 216.

Table 5 Training set, test set, and retraining set for the PGADI-HS smoother in AMG using the GPR(Example 5.2).

Training set	$n : 8 \sim 160, \Delta n = 4$	Test set	$n : 1 \sim 220, \Delta n = 1$	Retraining set	$n : 170 \sim 216, \Delta n = 10$

Fig. 2 Regression curves of (α, ω) with respect to n in the PGADI-HS smoothing algorithm of the AMG method(Example 5.2).

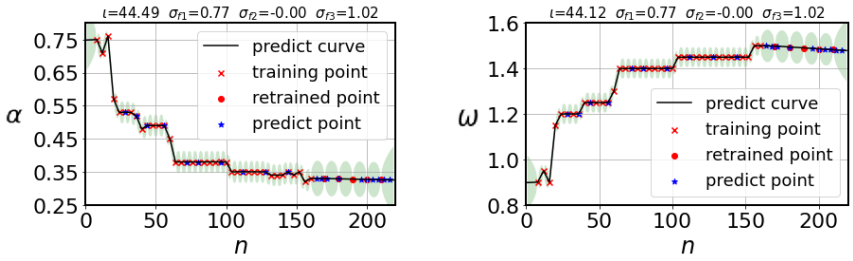

Here are the predicted results for a partial partition. The prediction indicates that α tends to approach 0.33 with a decreasing trend, while ω tends to approach 1.50 with an increasing trend. Clearly, by predicting the parameters, we have saved a significant amount of traversal time, and at the same time, we have achieved higher reliability compared to the empirical parameter selection.

Table 6 Prediction results using AMG the PGADI-HS smoother(Example 5.2).

n	(α, ω)	$iter$	$cputime$	n	(α, ω)	$iter$	$cputime$
28	(0.53,1.20)	9	0.017	36	(0.52,1.20)	10	0.025
44	(0.49,1.25)	12	0.046	56	(0.49,1.25)	12	0.072
72	(0.38,1.40)	22	0.366	80	(0.38,1.40)	23	0.444
96	(0.38,1.40)	25	0.567	112	(0.35,1.45)	28	1.241
128	(0.35,1.45)	36	2.728	144	(0.35,1.45)	38	3.768
164	(0.33,1.50)	44	5.815	168	(0.33,1.50)	44	5.995
172	(0.33,1.50)	44	6.737	180	(0.33,1.50)	44	7.216
196	(0.33,1.50)	47	8.882	200	(0.33,1.50)	49	10.717
204	(0.33,1.50)	49	10.943	208	(0.33,1.50)	50	11.196
212	(0.33,1.50)	50	11.371	216	(0.33,1.50)	50	11.853

Example 5.3 Consider the following equation [15]

$$\begin{cases} -\epsilon \Delta u + b \cdot \nabla u = f, & (x, y) \in \Omega = [0, 1] \times [0, 1], \\ u = 0, & (x, y) \in \partial\Omega. \end{cases}$$

The exact solution is given by $u = x(1-x)\sin(\pi y)$, with coefficients chosen as $\epsilon = 0.01$, $b = (\cos\varphi, \sin\varphi)^T$, and the right-hand side is derived from the exact solution. Except

for the preconditioning matrix, our setup for Example 5.3 is the same as for Example 5.1. For the preconditioning matrix, we choose the incomplete LU decomposition of A. Setting $\varphi = 0$, a simple traversal reveals that the algorithm is sensitive to the changes in both α and ω. After roughly determining the optimal parameter range through a coarse traversal, we will traverse to obtain the optimal parameters by setting α in the interval $(0, 0.8]$ with a step size of 0.01 and setting ω in the interval $(0.8, 1.8]$ with a step size of 0.05. The following are the comparative results using the PGADI-HS method and the PHSS method as smoothers:

Table 7 Comparison of the AMG methods with different smoothing algorithms(Example 5.3).

	PGADI-HS Method				HSS Method		
n	(α, ω)	*iter*	*cputime*	*traversal cputime*	α	*iter*	*cputime*
16	(0.03,0.50)	3	0.044	115.031	0.7144	3	0.314
32	(0.28,1.30)	3	1.941	4898.858	0.4861	4	2.640
48	(0.35,1.30)	4	26.275	40644.449	0.3410	5	38.809
64	(0.73,0.6)	4	104.572	208599.204	0.2449	8	196.908

Below, we use the GPR algorithm to predict the splitting parameters (α, ω). The following table provides the training set, test set, and retraining set for GPR. For small-scale linear systems, we obtain the training set with n ranging from 16 to 44 in steps of $\Delta n = 4$, and from 52 to 76 in steps of $\Delta n = 4$. For the test set, we select a step size of $\Delta n = 1$, with n ranging from 1 to 128. In the retraining set, we select a step size of $\Delta n = 4$, with n ranging from 30 to 128.

Table 8 Training set, test set, and retraining set for the GPR algorithm in the PGADI-HS smoothing method in AMG method (Example 5.3).

Training Set	$n : 16 \sim 44, \Delta n = 4$ $n : 52 \sim 76, \Delta n = 4$	Test Set	$n : 1 \sim 128, \Delta n = 1$	Retraining Set	$n : 30 \sim 128, \Delta n = 4$

Below are the predicted results for partial subdivisions, compared with the optimal parameters obtained by traversal, it is clear that the predicted parameters save a significant amount of time and computational cost.

Fig. 3 Regression curves of (α, ω) against n for the PGADI-HS smoothing method in AMG method(Example 5.3).

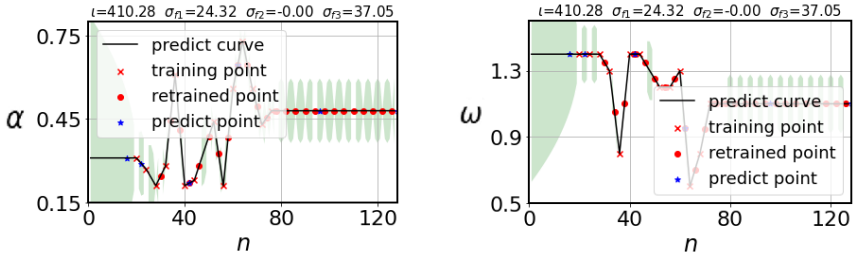

Table 9 Predicted results for solving Example 5.3 with the PGADI-HS method as the smoother in AMG method

n	(α, ω)	$iter$	$cputime$
16	(0.3099,1.39)	3	0.081
22	(0.2898,1.39)	3	0.245
42	(0.2200,1.40)	4	9.951
62	(0.6449,0.95)	5	94.445
96	(0.4796,1.10)	6	1209.240
128	(0.4798,1.09)	27	7660.879

In the Example 5.3, the advantage of predicted parameters is even more evident when dealing with large-scale linear systems. It first obtains a dataset from small-scale problems and then predicts the optimal parameters for solving large-scale linear systems. In this example, the overall time to obtain the dataset is even less than the time to traverse the optimal parameters at $n = 128$. Similarly, such advantages hold true for other examples when calculating at larger scales.

6 Summary

This paper presents a smoothing method for algebraic multigrid methods, which is based on the Practical GADI-HS approach within the GADI framework. We have found that this method effectively enhances the computational efficiency of algebraic multigrid methods. Finally, we propose a parameter selection method combined with GPR. When the scale of the linear algebraic system is sufficiently large, using GPR to predict parameters greatly saves time. In the end, we still have some interesting issues to be studied, such as how to choose the preconditioning matrix to speed up the computation, and extending the application of this smoothing algorithm to other linear algebraic systems, etc.

References

[1] R. E. Bank, T. Dupont, An optimal order process for solving finite element equations. Math. Comput. 1981, 36: 35-51.

[2] D. Braess, W. Hackbusch, A new convergence proof for the multigrid method including the V-cycle. SIAM J. Numer. Anal. 1983, 20: 967-975.

[3] J. H. Bramble, J. E. Pasciak, New estimates for multilevel algorithms including the V-cycle. Math. Comput. 1993, 60: 447-471.

[4] A. Brandt, Multi-level adaptive solutions to boundary-value problems. Math. Comput. 1977, 31: 333-390.

[5] S. C. Brenner, Convergence of the multigrid V-cycle algorithms for second order boundary value problems without full elliptic regularity. Math. Comput. 2002, 71: 507-525.

[6] C. C. Douglas, Multigrid algorithms with applications to elliptic boundary value problems. SIAM J. Numer. Anal. 1984, 21: 236-254.

[7] W. Hackbusch, Multigrid Methods and Applications. Springer, Berlin, 1985.

[8] J. Mandel, S. F. McCormick, R. E.Bank, Variational multigrid theory. In: Multigrid methods. Frontiers in Applied Mathematics, SIAM, Philadelphia, 1987.

[9] P. Wesseling, An introduction to multigrid methods. Pure and Applied Mathematics. Chichester, New York, 1992.

[10] R. E. Bank, A comparison of two multilevel iterative methods for nonsymmetric and indefinite elliptic finite element equations. SIAM J. Numer. Anal. 1981, 18: 724-743.

[11] J. H. Bramble, J. E. Pasciak, J. C. Xu, The analysis of multigrid algorithms for nonsymmetric and indefinite elliptic problems. Math. Comput. 1988, 51: 389-414.

[12] J. H. Bramble, D. Y. Kwak, J. E. Pasciak, Uniform convergence of multigrid V-cycle iterations for indefinite and nonsymmetric problems. SIAM J. Numer. Anal. 1994, 31: 1746-1763.

[13] J. Mandel, Multigrid convergence for nonsymmetric, indefinite variational problems and one smoothing step. Appl. Math. Comput. 1986, 19: 201-216.

[14] J. P. Wang, Convergence analysis of multigrid algorithms for nonselfadjoint and indefinite elliptic problems. SIAM J. Numer. Anal. 1993, 30: 275-285.

[15] S. S. Li and Z. D. Huang. Convergence analysis of HSS-multigrid methods for second-order nonselfadjoint elliptic problems, BIT, 53(4), 2013, 987-1012.

[16] J. W. Ruge, K. Stüben. Multigrid Methods. SIAM, 1987. 73-130.

[17] P. Bastian, M. Blatt, R. Scheichl, Algebraic multigrid for discontinuous Galerkin discretizations of heterogeneous elliptic problems. Numer. Linear Algebra Appl. 2012, 19(2): 367-388.

[18] F. Kickinger, Algebraic multi-grid for discrete elliptic second-order problems. Multigrid Methods V: Proceedings of the Fifth European Multigrid Conference held in Stuttgart, 1998, 157-172.

[19] C. Richter, S. Schöps, M. Clemens, GPU acceleration of algebraic multigrid preconditioners for discrete elliptic field problems. IEEE T. Magn. 2014, 50(2): 461-464.

[20] M. Brezina, R. Falgout, S. MacLachlan, T. Mccormick, S. Mccormick, J. Ruge, Adaptive Algebraic Multigrid. SIAM J. Sci. Comput. 2006, 27(4): 1261-1286.

[21] Y. Notay, An aggregation-based algebraic multigrid method. Electronic T. Numer. Anal. 2010, 37: 123-146.

[22] K. Jiang, X. Su, J. Zhang, A general alternating-direction implicit framework with Gaussian process regression parameter prediction for large sparse linear systems. SIAM J. Sci. Comput. 2022, 44(4): A1960-A1988.

[23] Z. Z. Bai, G. H. Golub, M. K. Ng, Hermitian and skew-Hermitian splitting methods for non-Hermitian positive definite linear systems. SIAM J. Matrix Anal. Appl. 2003, 24(3): 603-626.

[24] K. Jiang, Zhang J, Q. Zhou, Multitask kernel-learning parameter prediction method for solving time-dependent linear systems. CSIAM T. Appl. Math. 2023, 4(4): 672-695.

[25] A. H. Schatz, J. P. Wang, Some new error estimates for Ritz-Galerkin methods with minimal regularity assumptions. Math. Comput. 1996, 65: 19-27.

[26] J. F. Maitre, F. Musy, Multigrid methods: convergence theory in a variational framework. SIAM J. Numer. Anal. 1984, 21: 657-671.

[27] J. H. Bramble, X. J. Zhang, The analysis of multigrid methods. In: Handbook of Numerical Analysis VII, North-Holland, Amsterdam, 2000.

[28] I Luz, M Galun, H Maron, R Basri, I Yavneh. Learning algebraic multigrid using graph neural networks. InInternational Conference on Machine Learning 2020 Nov 21 (pp. 6489-6499). PMLR.

[29] P. F. Antonietti, M. Caldana and L. Dedè, Accelerating algebraic multigrid methods via artificial neural networks, Vietnam J. Math. 51(1), 2023, 1-36.